Polymer 51 (2010) 755–762

Contents lists available at ScienceDirect

Polymer

journal homepage: www.elsevier.com/locate/polymer

Thermomechanical characterization of a shape memory polymer based self-repairing syntactic foam

Guoqiang Li [a,b,*], Damon Nettles [a]

[a] Department of Mechanical Engineering, Louisiana State University, Baton Rouge, LA 70803, USA
[b] Department of Mechanical Engineering, Southern University, Baton Rouge, LA 70813, USA

ARTICLE INFO

Article history:
Received 24 September 2009
Received in revised form
30 November 2009
Accepted 5 December 2009
Available online 22 December 2009

Keywords:
Foam
Self-healing
Shape memory polymer

ABSTRACT

While the current self-healing approaches such as micro-capsules, hollow fibers, thermally reversible covalent bonds, ionomers, incorporation of thermoplastic particles, etc., are very effective in self-healing micro-length scale damage, self-healing of structural scale or macro-length scale damage remains one of the grand challenges facing the self-healing community. We believe that self-healing of structural damage may need multiple steps, at least two steps: close then heal (CTH), similar to the biological healing of wounds in the skin. In a previous study [1], it has been proven that the confined shape recovery functionality of a shape memory polymer (SMP) based syntactic foam can be utilized to repair structural damage such as impact damage repeatedly, efficiently, and almost autonomously. The purpose of this study is to investigate the effect of various design parameters on the closing efficiencies of both the pure SMP and the SMP based syntactic foam. A systematic test program is implemented, including glass transition temperature (T_g) determination by dynamic mechanical analysis (DMA), isothermal compressive constitutive behavior at various temperatures, and stress-controlled uniaxial compression programming and shape recovery. During thermomechanical cycle testing, two stress levels are utilized for programming and three confinement conditions (fully confined, partially confined, and free) are investigated for shape recovery. It is found that the programming stress is restored under confined recovery conditions, which helps in fully closing the crack; the foam shifts the T_g higher and increases the stiffness at temperatures above the T_g; higher programming stresses lead to slightly higher shape fixity but lower shape recovery in free recovery cases; a higher programming stress also results in a higher peak stress for confined recovery conditions; while the peak stress recovered is controlled by thermal stress, the final stress recovered is controlled by the programming stress, which is stored and recovered using an entropic mechanism. This study lays a solid foundation for using shape memory polymer based composites to self-repair macro-length scale damage.

1. Introduction

Self-healing of structural damage has been a tremendous interest in the scientific community recently [1–3]. The ability to heal wounds is one of the truly remarkable properties of biological systems. A significant challenge facing the materials science community is to design smart synthetic systems that can mimic this behavior by not only sensing the presence of a wound or defect, but also by actively re-establishing the continuity and integrity of the damaged area. Such self-healing materials would significantly extend the lifetime and utility of a vast array of manufactured structures [1–3].

Because of the widespread use of thermoset polymers in structural applications, self-healing of damage in thermosetting polymers has been a research focus for years. The first self-healing material utilized either micro-capsules [4,5] or hollow glass fibers [6], which enclosed a monomeric fluid, with catalysts dispersed throughout the matrix material. When a propagating crack encounters one of the dispersed capsules or hollow glass fibers, the capsule or fiber bursts or fractures and the encased fluid flows into the cracked region. Catalyst in the vicinity initiates an *in-situ* polymerization reaction such as ring-opening metathesis polymerization (ROMP) and thus patches the crack. While this repairing scheme leads to high efficiency in an autonomous fashion and at a molecular level, it cannot repair damage more than once. Some modified versions of this idea such as a self-healing system that simulates the human circulatory

* Corresponding author. Department of Mechanical Engineering, Louisiana State University, Baton Rouge, LA 70803, USA. Tel.: +1 225 578 5302; fax: +1 225 578 5924.
E-mail address: guoli@me.lsu.edu (G. Li).

0032-3861/$ – see front matter © 2009 Elsevier Ltd. All rights reserved.
doi:10.1016/j.polymer.2009.12.002

system (i.e., a micro-vascular system), have been developed and can self-heal damage more than once but face additional challenges such as unintentional discharge of healing agent due to ruptured flow channels, and potential depletion of the catalyst dispersed in the matrix after several rounds of healing [7]. Recent developments in self-healing thermosets include thermo-reversible covalent bonds [8], incorporation of thermoplastic particles [9,10], ionomers [11], etc. In general, these systems are very successful in self-healing micro-length scale damage. However, they face tremendous challenges when used to heal macro-length or structural damage, which is usually in the scale of millimeters. For example, using large capsules or thick hollow fibers may provide the large volume of healing agent required to heal a macroscopic crack, however they themselves may become a source of defects once the healing agent has been released. For thermo-reversible covalent bonds and ionomers, cracked surfaces must be brought in contact with each other before self-healing can take place. In the case of incorporating thermoplastic particles, the large amount needed to heal macroscopic damage may also adversely affect the strength and dimensional stability of the matrix.

We believe that we cannot burden one type of healing scheme too much. Healing of structural scale damage may need multiple schemes or steps. From biology we learn that healing takes at least two steps: 1) closing of a wound through clotting followed by 2) the gradual growth of new cells. To mimic biological systems, the self-healing of structural scale damage needs first to fill or close the crack before the existing self-healing schemes, such as microcapsules, can take effect. In other words, we advocate a two-step healing scheme: close then heal (CTH).

As a fast growing active material [12–14], we believe that shape memory polymers (SMPs) can be used to partially repair structural damage under confined shape recovery (i.e., the first step in the proposed CTH). The idea is that the SMP based structure first obtains its permanent shape (shape B) after curing [13]. Afterwards, the volume of the structure is reduced by compression through a process called programming. After programming, the structure has a temporary shape, or working shape (shape A), and is ready to be used. During service, some internal damage such as matrix cracking may be created by external loading such as an impact. When the damaged structure is heated, the SMP matrix remembers its original shape B and attempts to return to it. If this expansion is resisted by external confinement, the SMP matrix will be pushed towards any internal open space, such as crack damage. If the programming is designed appropriately, the cracks can be closed. Without the external confinement, the SMP matrix will recover its original shape B with little or no closure of the internal cracks [1]. Therefore, external confinement, along with compression programming, is the key in achieving self-closing. Fig. 1 demonstrates the proposed programming-closing process. It is noted that, while it seems that tension programming can also repair internal cracks during free shape recovery (the specimen becomes shorter and thus closes the crack), the free recovery changes the geometry of the structure or compromises the dimensional stability as the structure recovers to its original shape. If confined recovery is used after tension programming (i.e., if the dimensional stability is maintained), the internal crack cannot be closed because the material is not allowed to be pushed towards the internal open space (i.e., the crack). Therefore, compression programming is a better choice, as tension programming may not work.

It is envisioned that the shape recovery is directional (i.e., recovery occurs along the loading direction used during programming). Therefore, only cracks perpendicular to the loading direction can be effectively closed if 1-D confinement is used. However, if 3-D confinement is used, the crack can be closed regardless of its Mode (I, II, III, or mixed) or its orientation due to the volume recovery. In a previous study, a grid stiffened syntactic foam has been used as a sandwich core for enhancing post-impact residual strength [15,20]. In this design, the grid skeleton inherently provides in-plane confinement to the foam. If additional confinement, such as shape memory alloy z-pins are used, autonomous transverse confinement can also be obtained. Therefore, realization of 3-D confinement in practice is not a difficult task.

Because the shape recovery process is driven by conformational entropy and the only human intervention is direct or indirect heating, the closing process is almost autonomous. Also, the change between shape A and shape B accompanies a physical or geometrical change only, thus the programming-recovery cycle is repeatable. This basic idea has been shown in a previous study [1]. It has been demonstrated that a partially confined shape recovery of a SMP based syntactic foam can mend impact damage repeatedly,

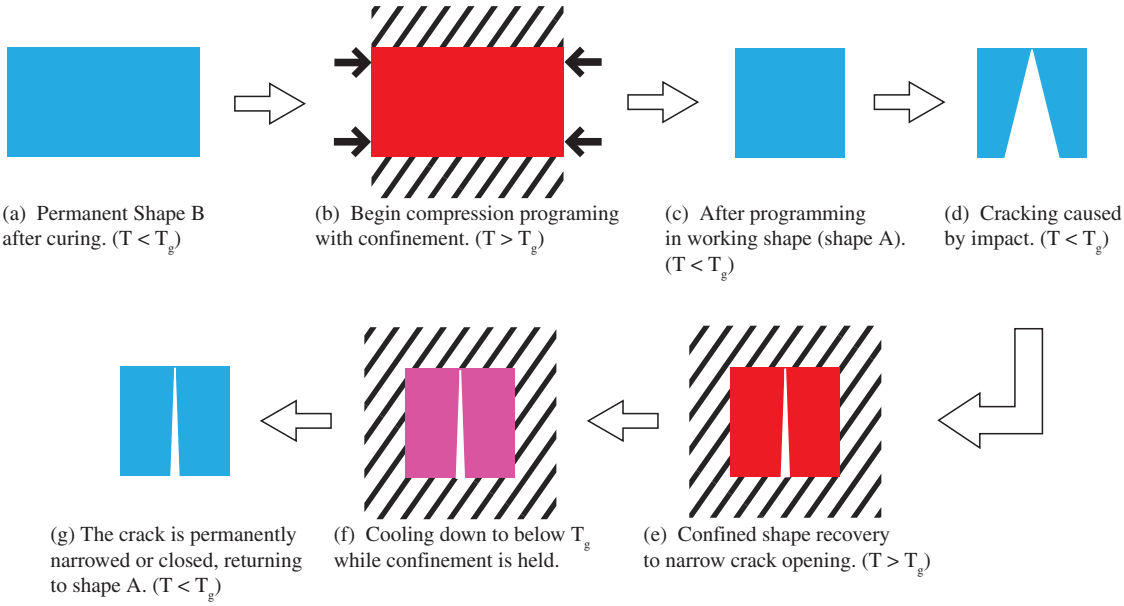

Fig. 1. Schematic of the self-closing scheme of the proposed smart foam (T_g is the glass transition temperature of the foam).

efficiently, and almost autonomously. We believe that the closing scheme in combination with a micro-length scale healing scheme such as micro-capsules or thermoplastic particles would achieve healing at the molecular-length scale, satisfying all the self-healing criteria: autonomously, repeatedly, efficiently, and at a molecular-length scale.

The objective of this study is to investigate the effect of various design parameters on the shape fixity and shape recovery of the self-closing syntactic foam, in particular, the effect of external confinement on the self-closing efficiency. It is anticipated that the results from this study will lay a solid foundation for better self-closing of the syntactic foam and a class of shape memory polymer based composite materials and structures.

2. Experimentation

2.1. Raw materials

The syntactic foam consists of hollow glass microspheres dispersed in a shape memory polymer matrix. The polymer is a styrene based thermoset SMP resin system ($T_g = 62\,^{\circ}C$) sold commercially by CRG Industries under the name *Veriflex*. The glass microballoons were purchased from Potters Industries (Q-CEL 6014: 85 μm average outer diameter, effective density of 0.14 g/cm^3, and 0.8 μm wall thickness). These raw materials have been used previously for the smart syntactic foam [1] and conventional epoxy based syntactic foams [15–17].

2.2. Specimen preparation

The SMP based syntactic foam was fabricated by dispersing 40% by volume of hollow glass microspheres into the SMP resin. The microspheres were added incrementally, with several minutes of mechanical blending between additions. A hardening agent was then added and the solution mixed for 10 min. The composite was poured into a $229 \times 229 \times 12.7$ mm steel mold and placed in a vacuum chamber at 40 kPa for 20 min in order to remove any air pockets introduced during the mixing process. Based on our previous study [1], we used the curing cycles shown in Table 1. After curing, the foam panel was de-molded and $30 \times 30 \times 12.7$ mm specimens were cut from the bulk for further testing.

2.3. DMA testing

The shape memory effect revolves around a temperature range centered at the glass transition temperature (T_g). Below this range the material is rigid and above it is in a rubbery-elastic state. Recovery must be done above the T_g in order to transform between shape B and A. DMA testing was conducted in order to determine the T_g of both the pure SMP and the syntactic foam. A single cantilever beam method was used on a DMA 2980 machine from TA Instruments. The SMP specimen size was $17.5 \times 11.9 \times 1.20$ mm and the foam was $17.5 \times 12.1 \times 1.73$ mm. The temperature was ramped from room temperature to 120 °C at a rate of 3 °C/min, with a frequency of 1 Hz, and an amplitude of 15 μm. The storage modulus curve was used to determine the T_g as suggested by ASTM E 1640-04.

Table 1
Curing cycle for the pure SMP and SMP based syntactic foam.

Temperature	79 °C	107 °C	121 °C
Pure SMP	24 h	6 h	–
Foam	24 h	3 h	9 h

2.4. Isothermal stress–strain behavior

Flat-wise compression was performed on a MTS QTEST/150 electromechanical frame outfitted with a moveable furnace per the ASTM C 365 standard. Stress–strain responses were generated for room temperature and two temperatures above the T_g (79 °C and 121 °C). Specimens were placed in the preheated furnace and at least 30 min was allowed for temperature equilibration. Compression was then conducted in a strain-controlled manner at a constant rate of 1.3 mm/min to a strain level of 60%.

2.5. 1-D stress-controlled compression programming

In order to determine the effect that stress and strain levels have on shape memory performance and to observe how microstructural changes influence thermomechanical behavior, two stress levels were chosen: 47 kPa and 263 kPa. Stress-controlled programming was conducted using a linear variable differential transducer (LVDT) in conjunction with a compression fixture, weights, and a forced convection heating chamber (Fig. 2). The top of the fixture (and any additional weight) was suspended and everything but the specimen was preheated to 79 °C. The specimen was introduced into the system and allowed to equilibrate for 45 min. Flat-wise compression was achieved by lowering the suspended weight onto the specimen. Approximately 25 min were allowed for the deformation to stabilize. This completed the first step (prestrain) of the programming. In step 2 (cooling), the heating was first stopped, and the system was allowed to naturally cool to room temperature while maintaining the stress level. The LVDT tracked the movement of the specimen during this cooling step. Once room temperature was reached, the specimen was unloaded (step 3). This completed the three-step stress-controlled thermomechanical programming.

2.6. Shape recovery

In order to investigate the effect of external confinement on the shape recovery or self-closing efficiency, three different external confinements were used: fully confined, partially confined, and free. Due to limitations of the MTS machine used, partially confined

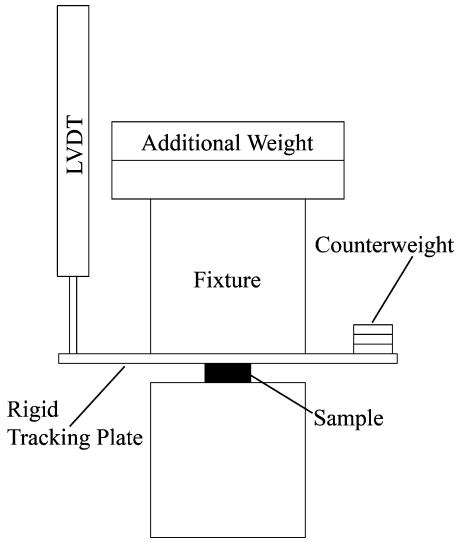

Fig. 2. Setup used for the stress-controlled programming consisting of an LVDT, fixture, and weights. A static load was used to compress the specimen and the deformation measured using the LVDT.

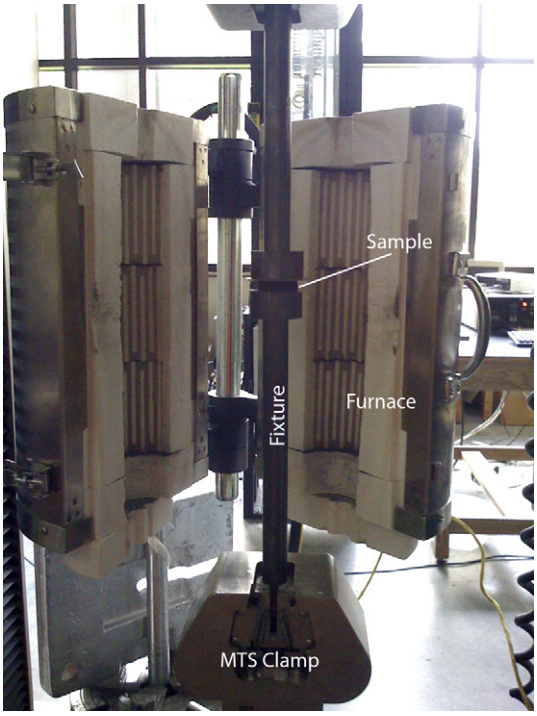

Fig. 3. MTS machine with furnace and fixture used for fully-confined recovery. The fixture provided 1-D external confinement and the furnace used to trigger the shape memory effect by heating the specimen above its T_g. The MTS machine was used to record the resulting recovery stress.

shape recovery was not determined through the thermomechanical recovery test; rather, it was conducted through direct observation under a SEM.

Fully confined recovery was performed using the MTS machine and furnace. Once the specimens were programmed under stress-controlled conditions, as described above, they were placed in the fixture shown in Fig. 3 such that the strain was fixed and the stress was initially zero. Heating was performed at an average rate of 0.3 °C/min from room temperature until 79 °C and then held for approximately 20 min (some specimens were held for over 24 h in order to investigate the stress relaxation behavior.). The MTS machine's load cell was used to record the recovered force as a function of time and temperature.

Stress-controlled (partially confined) recovery was conducted using the setup shown in Fig. 2, but without the LVDT. A specimen was first programmed under stress-controlled conditions. Then, its cross section was exposed and an artificial crack was generated in a direction perpendicular to the programming axis using a sharp blade. A SEM was used to catalog this damage. The specimen was then returned to the heating chamber and a constant uniaxial compressive stress equivalent (in both magnitude and direction) to that used during programming was applied. The temperature was set to 79 °C and the specimen was allowed to soak for 3 h while maintaining the load. It was then slowly cooled to room temperature and unloaded. The cross section of the specimen was again imaged under the SEM in order to evaluate the closing efficiency.

Stress-free recovery was implemented on programmed specimens by placing them in a heating chamber with no load. The temperature was ramped quickly from room temperature to 49 °C and allowed to soak for 20 min. It was then ramped from 49 to 77 °C at a rate of 0.16 °C/min in order to capture the strain change with temperature, before finally being set to 79 °C for 30 min.

3. Results and discussion

3.1. DMA test results

The storage modulus and loss modulus of the pure SMP and the SMP based syntactic foam are shown in Fig. 4. The glass transition region was determined using the storage modulus curve, as is suggested in ASTM E 1640-04. The intersection of tangent lines below the onset of the transition and to the inflection points denotes the upper and lower limits of the glass transition zone, with the average value in between determining the T_g.

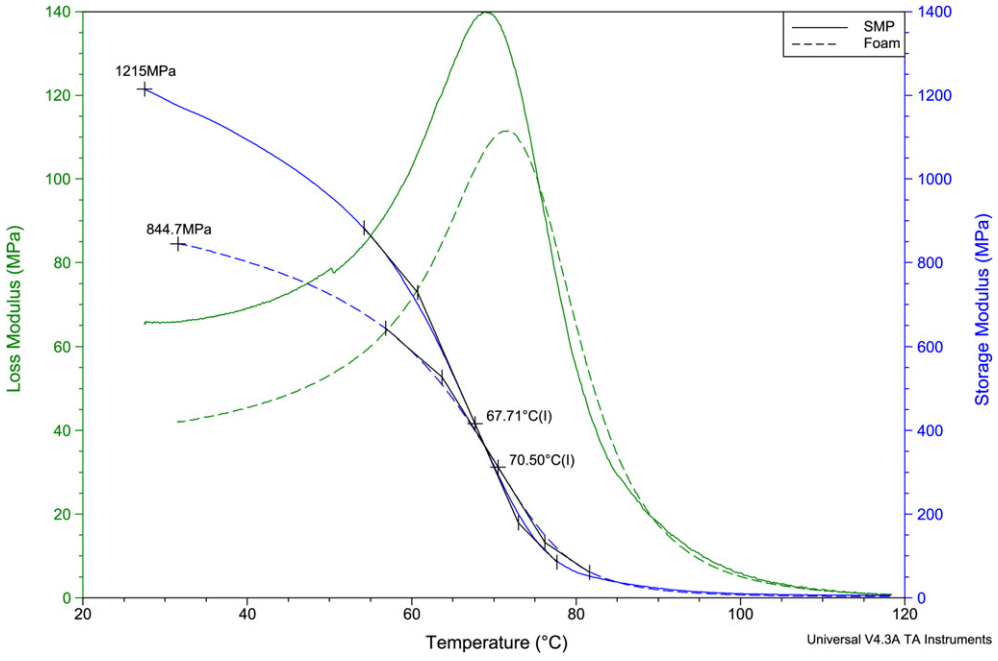

Fig. 4. DMA results for the pure SMP and syntactic foam. The T_g regions were determined from the storage modulus curves.

For the pure SMP, we obtained a glass transition zone range from 60.73 to 73.00 °C with a $T_g = 67.71$ °C. The manufacturer lists a value of $T_g = 62$ °C as determined by differential scanning calorimetry (DSC). This is about 4 °C lower than results obtained from their DMA tests, consistent with our results. In the foam, we observed a shift up about 2.8 °C in the glass transition region to 63.69–76.19 °C with a $T_g = 70.50$ °C. This shift may be caused by the addition of the glass microspheres, which may have increased the T_g of the SMP immediately surrounding them through physical adsorption or chemical reactions, restricting the mobility of the SMP molecules.

In order to perform efficient programming and shape recovery tests, we must work above the T_g region where the switching phase is activated. Therefore, we chose 79 °C as a testing temperature since it is just above the upper limit of the T_g region in the foam.

3.2. Isothermal stress–strain behavior

Fig. 5 shows the stress–strain response of the pure SMP and syntactic foam under uniaxial flat-wise compression at room temperature. The foam displays three distinct regions relating to microstructural changes. Region 1 (up to 5% strain) contains the linear elastic portion governed by microsphere cell wall bending and stretching. After the yield point we enter region 2 (5–40% strain). The curve plateaus as microsphere cell walls are damaged from crushing and fracture. In region 3 (>40% strain) the crushed microspheres are densified and the foam is consolidated, leading to a quick growth in stress [18]. These microstructural changes are shown in the SEM images taken after 5, 30, and 60% strain. Also, it is seen that both the yield strength and the modulus of elasticity of the foam is lower than those of the pure SMP. This observation agrees with conventional syntactic foams [17].

As the temperature increases, the polymer chains become more ductile leading to reductions in the moduli and yield strength for both the pure SMP and foam. This behavior is particularly pronounced at temperatures higher than the T_g. Fig. 6 shows the stress–strain responses at 79 °C, just above the T_g region. There is approximately a 97% reduction in the yield strength of the foam compared to room temperature and that of the pure SMP behaves like a rubber, obscuring the yield point. When the temperature is increased to 121 °C, even the foam tends to behave like a rubber, as evidenced by the near disappearance of the yield point (see Fig. 6). However, we notice that at a temperature higher than the T_g, the foam shows higher yield strength (at 79 °C) and higher stiffness (at both 79 °C and 121 °C) than the pure SMP, which is opposite to the behavior at room temperature (below T_g). This is obviously due to the SMP's change from the glassy state below the T_g to the rubbery state above the T_g. In the rubbery state, addition of stiffer particles (such as glass microspheres) increases the stiffness and yield strength of the composite foam.

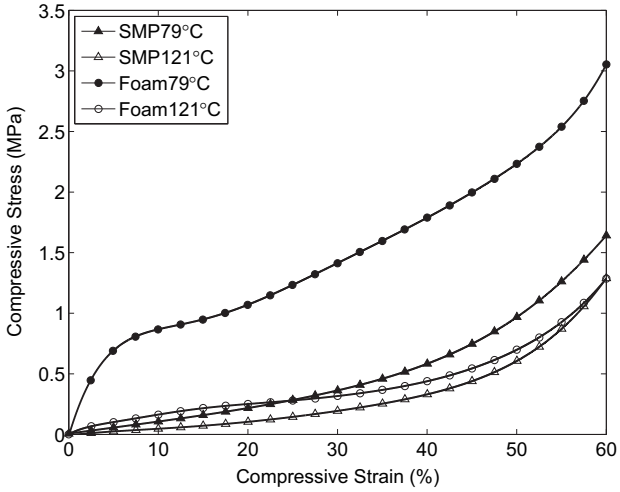

Fig. 6. Stress–strain curves for the pure SMP and syntactic foam at 79 °C and 121 °C. At temperatures above the T_g, the stiffness and strength were significantly lower. The foam was less affected due to the inclusion of microspheres.

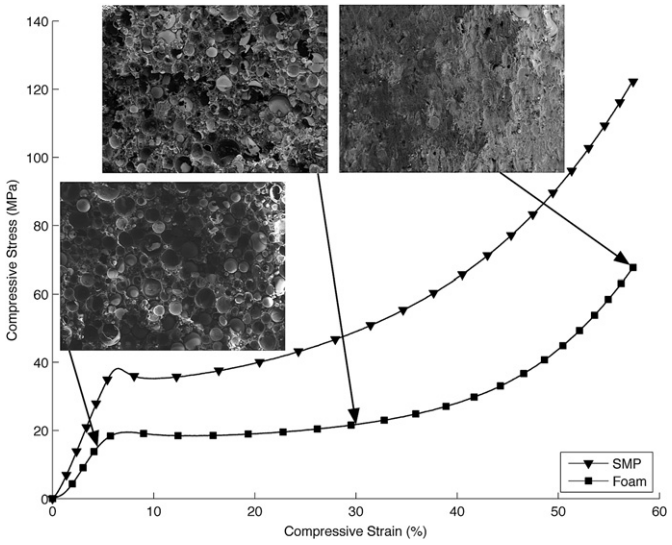

Fig. 5. Stress–strain response of the pure SMP and syntactic foam at room temperature. The SEM images show the microstructure of the foam at compressive strain levels of 5, 30, and 60%. A progressive breaking of the microspheres occurs as the strain level is increased.

3.3. 1-D stress-controlled programming and multiple recovery conditions

3.3.1. Free recovery

Typical three-step stress-controlled programming at stress levels of 263 kPa and 47 kPa, and free shape recovery for both the pure SMP and the foam are respectively shown in Figs. 7 and 8. The

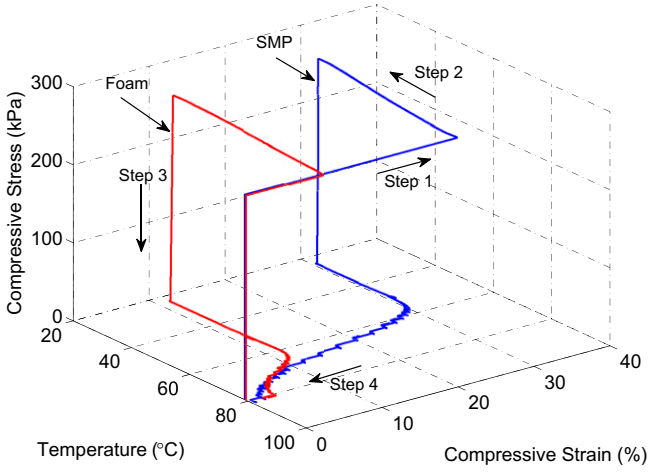

Fig. 7. Four-step thermomechanical cycles (high temperature loading → cooling → room temperature unloading → recovery) for the pure SMP and syntactic foam programmed under a stress-controlled condition with a prestress of 263 kPa at 79 °C followed by free recovery.

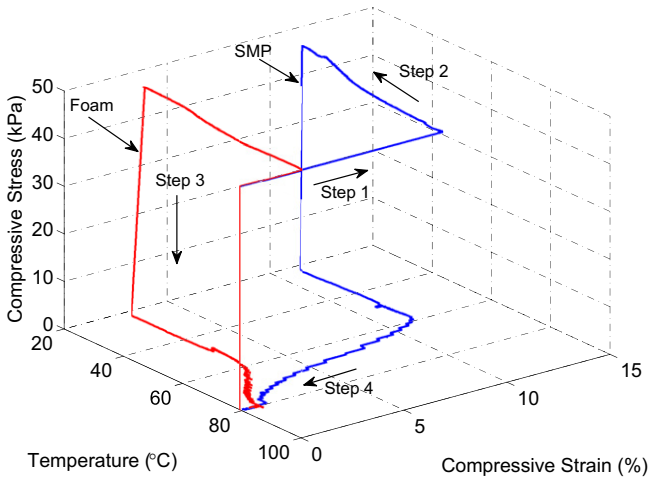

Fig. 8. Four-step thermomechanical cycles (high temperature loading → cooling → room temperature unloading → recovery) for the pure SMP and syntactic foam programmed under a stress-controlled condition with a prestress of 47 kPa at 79 °C followed by free recovery.

programming consists of a high temperature loading (step 1), followed by cooling (step 2) during which time the stress is held constant, and unloading at room temperature (step 3). Step 4 is a free recovery step whereby the programmed specimen is reheated to 79 °C and soaked for about 30 min. These four steps complete a thermomechanical cycle. The purpose of the programming is to fix a specimen in its temporary shape where it can be utilized. In step 1, the strain initially increases rapidly upon loading. Because the total load was applied to the specimen instantly at 79 °C and held, step 1 is represented by a stepped curve instead of a continuous function. The applied prestress in step 1 is held about 30 min at a temperature above the T_g, which allows creep to develop. This is why the compressive strain at the end of step 1 is higher than the strain at the same stress level from the isothermal compressive stress–strain curve shown in Fig. 6, which has no creep deformation. The subplot in Fig. 9 highlights this creep behavior for the foam at a constant stress of 263 kPa. In step 2, there is also a gradual

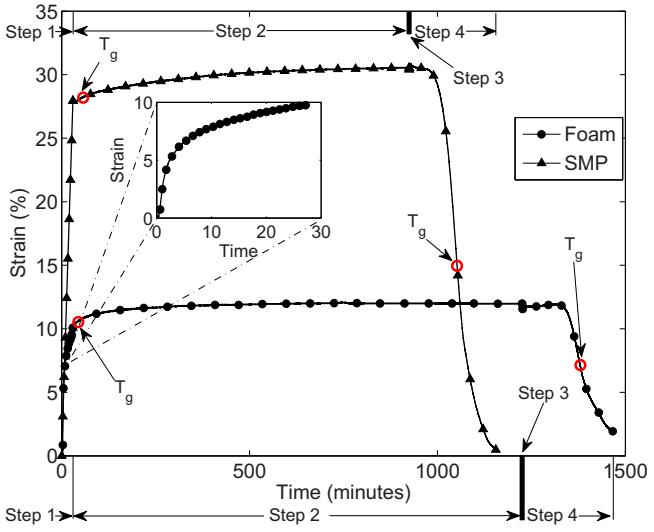

Fig. 9. Strain vs. time representation of the stress-controlled programming performed at 263 kPa followed by free recovery. The creep effect in the foam during step 1 is shown in the subplot.

increase of strain caused by thermal contraction, viscoelasticity (creep) in the T_g region, and viscoplasticity below the T_g region. It is interesting to note that in the foam, there may be a thin layer of SMP which has been absorbed by the glass microballoons. Because of the reduced mobility of the SMP within this layer, the overall T_g of the foam is increased, as shown in Fig. 4. Therefore, the actual T_g within this layer may be well above the average T_g shown because of its small volume. Similar behavior was found in carbon nanotube reinforced SMP composites [19]. Because of the increased T_g of this layer, some of the deformation in the T_g region in Fig. 9 may be in the form of viscoplasticity, while the SMP outside of this layer deforms viscoelastically. In step 3, the applied load is removed, leading to springback of the specimen, or a reduction in the compressive strain. The strain maintained at the end of step 3 is the permanent strain stored due to programming. In step 4, which is a free recovery step driven by conformational entropy, most of the stored strain is released. From Figs. 7 and 8 we see that the majority of the strain recovery occurs within the glass transition region once the switching phase has been activated.

Shape fixity and shape recovery values were calculated based on the thermomechanical cycles per [13]. The results are summarized in Table 2. The shape fixity for both the foam and the pure SMP is close to 100%. This is due to the small stress applied during the programming and high stiffness of the material at room temperature when the stress is removed, leading to a very small springback. The 263 kPa prestress makes the specimen denser and stiffer than the 47 kPa prestress does, leading to smaller springback and higher shape fixity. For the shape recovery, the pure SMP is still able to recover almost all the stored strain. The foam's shape recovery, however, has been reduced due to unrecoverable viscoplastic deformation below the T_g region. It may also include viscoplastic deformation within the T_g region for the interfacial transition zone confined by the glass microballoons. Also, the incorporation of microballoons may provide additional local intermolecular resistance to segmental rotation, and thus higher viscoplastic deformation, leading to a lower shape recovery than the pure SMP.

In order to better understand the rate of change of strain during the thermomechanical cycle, changes of strain with time are shown in Fig. 9 at a prestress of 263 kPa and in Fig. 10 at a prestress of 47 kPa. In step 1, the strain develops rapidly upon loading, gradually tapering off as creep progresses. The creep with time in step 1 is highlighted in the subplot in Fig. 9. In step 2, the change of strain with time can be divided into two regions. For the region around the T_g, the material continuously experiences creep, as represented by the curve with varying curvature. Below the T_g, the material is glassy and the change of strain is primarily due to thermal contraction, as evidenced by an almost straight line with constant slope. There is an increase in compressive stain of a few percent due to creep, viscoplastic deformation, and thermal contractions during cooling. In step 3, the unloading occurs suddenly. This step is actually a point in Figs. 9 and 10. Again, due to the relatively small stress applied and the large stiffness of the materials at room temperature, the springback is very small. In step 4, the strain recovery occurs primarily in the glass transition region.

Table 2
Shape fixity and recovery values for the pure SMP and SMP based syntactic foam under stress-controlled programming and free shape recovery at 79 °C.

Material	Stress (kPa)	Strain (%)	Fixity (%)	Recovery (%)
Pure SMP	47	11	98.5 ± 3.7	98.7 ± 3.8
	263	30	99.6 ± 1.4	98.4 ± 1.4
Foam	47	3	81.2 ± 11.8	87.6 ± 11.7
	263	12	96.7 ± 3.5	83.9 ± 3.0

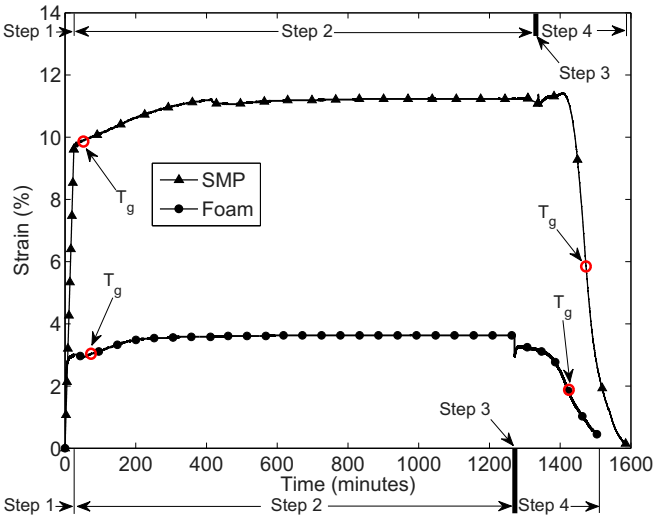

Fig. 10. Strain vs. time representation of the stress-controlled programming performed at 47 kPa followed by free recovery.

3.3.2. *Fully-confined recovery*

Since the programming is the same for the free recovery specimens and fully-confined specimens, our focus will be on step 4 of the thermomechanical cycles. The stress-temperature behavior under a fully confined recovery condition is shown in Fig. 11 for the two programming stresses (47 kPa and 263 kPa). The recovery stress–time behavior of the foam programmed by 47 kPa prestress is also highlighted by the subplot in Fig. 11. The recovery stress comes from two parts: thermal expansion stress and entropically stored stress. Since this is a 1-D fully confined recovery, the thermal stress can be calculated as: $\sigma = E\alpha\Delta T$, where σ is the thermal stress, E is the modulus, α is the coefficient of thermal expansion, and ΔT is the temperature change. When the temperature is below the T_g, the modulus is high. As the temperature rises, the stress increases until the temperature reaches the start of the glass transition region. Here, the stress shows a peak. While the coefficient of thermal expansion may still increase within the glass transition zone, the E decreases sharply, leading to a continuous reduction in stress. Once the temperature approaches the programming temperature (79 °C), the stress shows some relaxation initially (see the stress-time behavior inset for the foam programmed with 47 kPa in Fig. 11).

However, for a prolonged time period of near 24 hrs, the stress does not appreciably decrease further. From the test results, it is found that the final recovery stress is 258.9 kPa for the SMP and 221.8 kPa for the foam, for a programming stress of 263 kPa. However, when the programming stress is 47 kPa, the final recovered stress is 51.5 kPa for the pure SMP and 69.5 kPa for the foam (higher than the programming stress). This abnormal behavior may be due to the expansion of the fixture during the shape recovery process, which applied a compressive stress to the specimen during heating. While the specimens programmed using a 263 kPa prestress experienced similar conditions, the results are not as sensitive as the 47 kPa programmed specimens because the 263 kPa prestress produced a strain in the specimens much higher than the small additional strain caused by the expansion of the fixture. Therefore, the effect on the 263 kPa prestress programmed specimens is insignificant.

Comparing the recovery stress of the foam with the pure SMP, it is clear that (1) the foam has a higher peak stress than the pure SMP. This is because the foam has a higher modulus than the SMP at higher temperatures. (2) The temperature corresponding to the

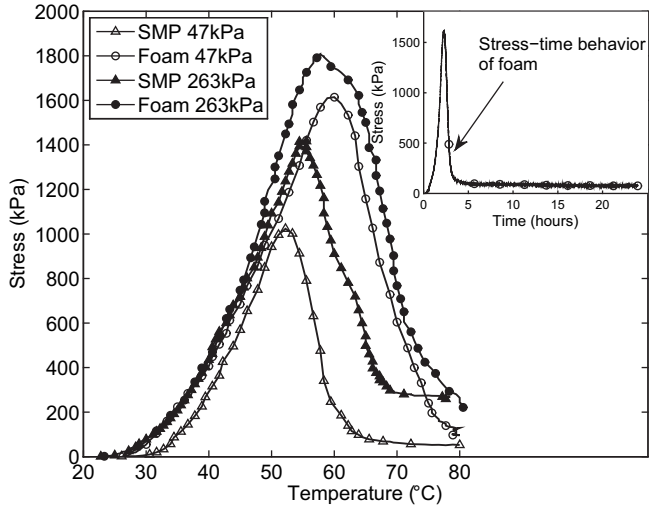

Fig. 11. Recovery under a fully confined condition. The recovered stress for the pure SMP and foam after stress-controlled programming with two prestresses is shown. The inset shows the long-term stress relaxation of the foam programmed by a 47 kPa compressive stress.

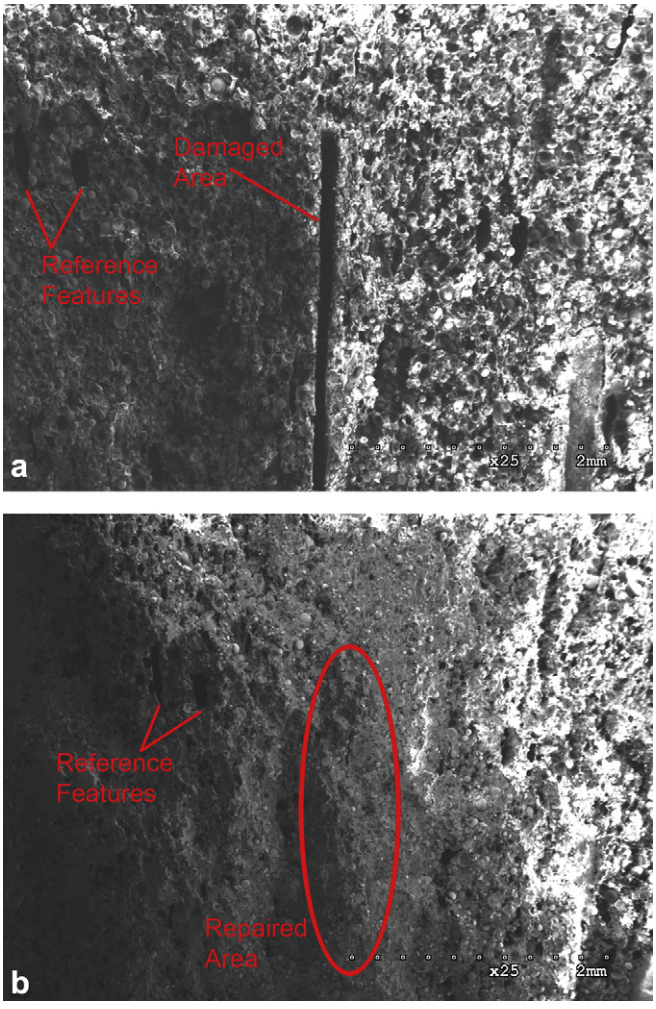

Fig. 12. a) SEM image of the cross section of a stress-controlled programmed specimen after damage has been generated. Programming was performed in a direction perpendicular to the crack. b) The same region after a partially-confined recovery showing the closing effect. Recovery occurred along the programming axis. Reference features already present in the specimen were chosen to aid in locating the damaged region.

peak stress is higher for the foam than for the SMP. This is in agreement with the T_g test results. (3) The peak stress in specimens programmed by a 263 kPa prestress is higher than in specimens programmed by a 47 kPa prestress. This is because the 263 kPa prestress makes the specimens denser and stiffer producing a quicker build up of thermal stress during heating and ultimately a higher peak stress.

3.3.3. Partially-confined recovery

The results for partially confined recovery are represented by direct SEM observation. As discussed previously in Section 2.6, the specimen was recovered under a constant stress equivalent to that used during programming. SEM observations of the foam before and after recovery are presented in Fig. 12 (a) and (b). During recovery there was an external stress constantly applied along the programming axis, which counteracts the internal entropically stored stress. Therefore, the specimen cannot recover to its original permanent shape. Instead, due to the external confinement, the recovered stress pushes the cracked surfaces into the empty space left by the artificial crack. They show effective closing of the artificial crack, suggesting that confined shape recovery of the SMP based syntactic foam is a way to close structural scale damage. We anticipate that a fully confined recovery condition would be even more effective at closing cracks regardless their modes or orientations since the 3-D confinement would provide a more stable frame for the recovered stress to act against.

4. Conclusion

Based on the test results, we draw the following conclusions:

- Confined shape recovery can fully close internal cracks.
- SMPs are a type of material that can be taught or trained. Its shape recovery functionality depends on the programming and method of recovery used.
- For free recovery, higher programming stress leads to higher shape fixity but lower shape recovery, which suggests that the prestress or prestrain level must be within a certain limit during programming in order to maximize the shape recovery functionality of the SMP and the SMP based syntactic foam.
- Although the peak stress during the confined recovery is determined by thermal expansion and is very high compared to the programming stress, the final stress recovered is dependent on the entropically stored stress and is close to the stress used for the stress-controlled programming.
- As compared to the pure SMP, the SMP based syntactic foam shifts the T_g upwards, possibly due to the existence of an interfacial transition zone with confined mobility, and increases the stiffness at higher temperatures. Even at a temperature of 79 °C, which is slightly above the T_g, the SMP and foam show a certain viscoelasticity, as evidenced by the creep during the programming and stress relaxation during the confined shape recovery. Also, viscoplasticity may be present due to the higher T_g in the interfacial transition zone.

Acknowledgements

This study was sponsored by the NASA/EPSCoR project under grant number NASA/LEQSF (2007-10)-Phase3-01 and NSF under grant number CMMI-0900064. The authors would also like to thank Mr. Wei Xu, Mr. Hari Konka, Dr. Kun Lian, and the CAMD facility for their help in acquiring the DMA results, Mr. Manu John for his experience and guidance working with these materials, and Mr. Naveen Uppu for his laboratory assistance.

References

[1] Li G, John M. Composites Science and Technology 2008;68:3337–43.
[2] Gould P. Materials Today 2003;6:44–9.
[3] Balazs AC. Materials Today 2007;10:18–23.
[4] Blaiszik BJ, Sottos NR, White SR. Composites Science and Technology 2008;68:978–86.
[5] White SR, Sottos NR, Geubelle PH, Moore JS, Kessler MR, Sriram SR, et al. Nature 2001;409:794–7.
[6] Pang JWC, Bond IP. Composites Science and Technology 2005;65:1791–9.
[7] Toohey KS, Sottos NR, Lewis JA, Moore JS, White SR. Nature Materials 2007;6:581–6.
[8] Liu YL, Chen YW. Macromolecular Chemistry and Physics 2007;208:224–32.
[9] Zako M, Takano N. Journal of Intelligent Material Systems and Structures 1999;10:836–41.
[10] Hayes SA, Jones FR, Marshiya K, Zhang W. Composites Part A-Applied Science and Manufacturing 2007;38:1116–20.
[11] Varley RJ, van der Zwaag S. Acta Materialia 2008;56:5737–50.
[12] Lendlein A, Jiang H, Jünger O, Langer R. Nature 2005;434:879–82.
[13] Behl M, Lendlein A. Materials Today 2007;10:20–8.
[14] Ratna D, Karger-Kocsis J. Journal of Materials Science 2008;43:254–69.
[15] Li G, Muthyala VD. Composites Science and Technology 2008;68:2078–84.
[16] Li G, John M. Materials Science and Engineering A 2008;474:390–9.
[17] Li G, Nji J. Composites Part A: Applied Science and Manufacturing 2007;38:1483–92.
[18] Eaves D. Handbook of polymer foams. United Kingdom: Rapra Technology Limited; 2004 [Chapter 1].
[19] Berriot J, Montes H, Lequeux F, Long D, Sotta P. Europhysics Letters 2003;64:50–6.
[20] Li G, Chakka VS. Composites Part A: Applied Science and Manufacturing 2010;41:177–84.